ChemComm

COMMUNICATION

View Article Online
View Journal | View Issue

Cite this: *Chem. Commun.*, 2024, **60**, 5638

Received 30th October 2023,
Accepted 23rd April 2024

DOI: 10.1039/d3cc05268k

rsc.li/chemcomm

Pseudoaromaticity-driven, transition metal detection by squaraine-derived enol phosphonium ylide chemodosimeters†

Raïssa Twiringiyimana and Brandon L. Ashfeld *

The addition of P^nBu_3 to *o*-substituted dianiline squaraine dyes leads to bench stable ylides. Exposure to a metal analyte in solution, results in P^{III} abstraction and rapid disruption of the ylide conjugation to promote reversion back to the squaraine dye giving an immediate turn-on colorimetric response. The stoichiometric sensitivity and accessibility of these chemodosimeters constitute effective organic dyes for trace transition metal detection.

Dianiline squaraines are colorful organic dyes utilized in non-invasive bio-imaging,[1] photovoltaics,[2] and ion-sensing.[3] They are characterized by two *para*-substituted electron donating anilines in a 1,3-orientation across an electrophilic, cyclobutadione core, resulting in a donor–acceptor–donor resonance stabilization effect.[3] However, the electrophilicity of the squaraine core renders it susceptible to nucleophiles present in biological systems, and is a frequent obstacle in fluorescence imaging.[4] This has led to a number of elegant macromolecular protection strategies to minimize the addition of exogenous nucleophiles and quenching of the squaraine dye.[5] While these approaches have proven effective at protecting the squaraine core and rendering the composite complex stable to biologically relevant environments, few studies have sought to exploit its inherent electrophilicity in the templated design of new chromophoric sensing agents.[6]

We recently sought to exploit the inherent electrophilicity of squaraine dyes in the design of new chemodosimeters wherein the addition of phosphine leads to stable, zwitterionic complex that serves as a positive response "turn on" sensor for the detection of specific trace analytes in solution (Fig. 1a).[6a] The phosphine-squaraine adducts **2** were effective as colorimetric sensors for transition metals such as Rh^I, Pd^{II}, Ir^I, and Au^I.[6a] However, one limitation of our initial design was that the adducts underwent only 1% reversion to the parent dye **1** despite an excess of the analyte present, thereby limiting the sensitivity of this class of indicators. Hence, we sought an alternative squaraine-based design that would ultimately result in a more dramatic positive response to the transition metal analyte. Herein, we introduce the successful identification of a rather unusual, highly conjugated phosphonium-based platform that is exceptionally stable and chemoselective for the detection of trace transition metals with a substantially more pronounced propensity to undergo complete reversion to the parent squaraine dye.

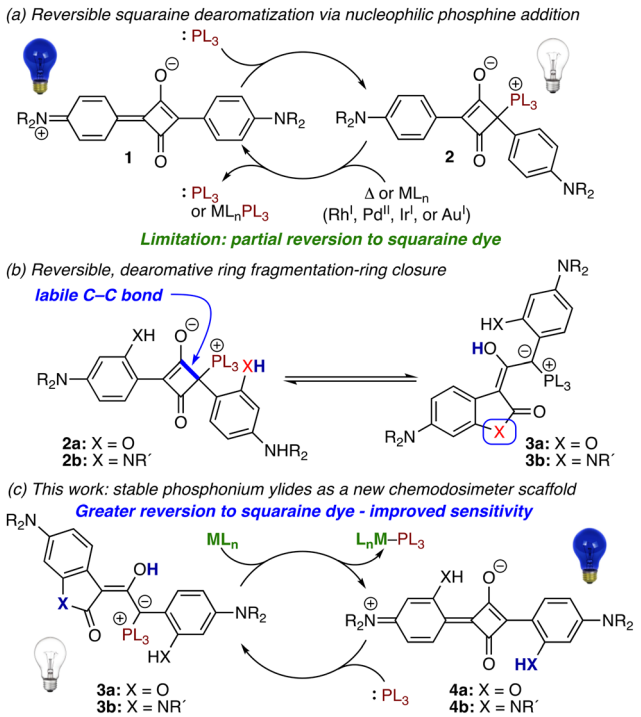

Fig. 1 Addition of phosphorus (III) to dianiline squaraines. (a) Colorimetric sensors for trace metals. (b) Reversion to squaraine dyes *via* Brønsted acid. (c) Reversion to squaraine dyes through metal-induced process.

Recently, we reported the dearomative skeletal reorganization of phosphine-squaraine adduct **2a**, derived from the addition of

Department of Chemistry and Biochemistry, University of Notre Dame, IN 46556, USA. E-mail: bashfeld@nd.edu

† Electronic supplementary information (ESI) available. See DOI: https://doi.org/10.1039/d3cc05268k

$^{n}Bu_3P$ to the corresponding dianiline squaraine bearing a hydroxy group vicinal to the four-membered ring, to benzofuranone **3a** (Fig. 1b).[7] Employing squaraines with an *N*-acyl group in place of the *o*-OH provided oxindole **3b** wherein the enhanced acidity of the *N*-acyl proton was critical to accessing the rearranged product.[7,8] A notable feature of these frameworks is the exceptionally stable enol and phosphorus ylide motifs afforded by the high degree of extended conjugation. Over the course of our study, we observed that while unreactive to various nucleophilic and electrophilic reagents, adducts **3** underwent reversion to the parent squaraine **4** in the presence of a Brønsted acid, presumably driven by the pseudo-rearomatization of the squaraine core. This observation led us to speculate on the propensity of phosphine adducts **3** to undergo complete and rapid reversion to the parent squaraine in the presence of an analyte capable of extracting $P^{n}Bu_3$ leading to more sensitive and efficient chemodosimeters for latent metal detection than our previous design (Fig. 1c).[7] Herein, we report the development of a thermally stable, stoichiometric colorimetric chemodosimeter for trace metal recognition.

We began our evaluation of ylides **3** as colorimetric chemodosimeters by assessing the extent of squaraine **4** formation in the presence of a transition metal complex.[6a] Construction of ylides **3a** and **3b** was accomplished following our previous report by treatment of *o*-substituted squaraines **4a** and **4b**, independently, with $P^{n}Bu_3$ to rapidly (*ca.* ~5 min) provide the desired heterocyclic frameworks in high yield (Scheme 1).[7] Our initial set of experiments toward evaluating the efficacy of ylides **3a** and **3b** as chemodosimeters consisted of assessing the extent to which squaraine dyes **4a** and **4b** underwent regeneration upon treatment with $[Rh(COD)Cl]_2$, $[Ir(COD)Cl]_2$, $Pd(OAc)_2$, $Au(PPh)_3Cl$ and $Rh(PPh_3)_3Cl$. Using ^1H NMR to track the conversion of **3a** to **4a**, exposure to 1 equiv. of $[Rh(COD)Cl]_2$, $[Ir(COD)Cl]_2$, and $Pd(OAc)_2$, independently, resulted in complete conversion to dye **4a** (Fig. 2). While the addition of $Au(PPh_3)Cl$ and $Rh(PPh_3)_3Cl$ to **3a** resulted in significant dye regeneration, and were substantially more responsive than our original phosphine squaraine adducts **2**, the 9 : 1 and 5 : 1 ratios of **4a:3a**, respectively, indicated a metal selective response. Similarly, the addition of $[Rh(COD)Cl]_2$, $[Ir(COD)Cl]_2$, and $Pd(OAc)_2$ to *N*-acyl oxindole **3b** resulted in complete conversion to squaraine **4b**, while exposure to $Au(PPh_3)Cl$ and $Rh(PPh_3)_3Cl$ to **3b** led to less dye formation, providing **4b : 3b** in 4 : 1 and 2 : 1 ratios, respectively (Fig. 3).

The disparate responses observed with $[Rh(COD)Cl]_2$, $[Ir(COD)Cl]_2$, and $Pd(OAc)_2$ relative to $Au(PPh_3)Cl$ and $Rh(PPh_3)_3Cl$ for ylides **3a/b** are likely due to the coordination capabilities of

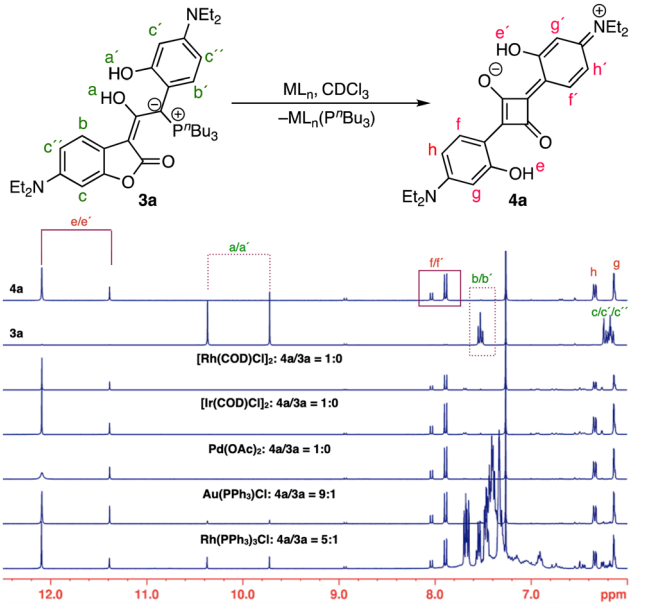

Fig. 2 Partial ^1H NMR spectra (500 MHz, $CDCl_3$) that illustrates conversion of **3a** (0.02 M) to **4a** upon addition of ML_n (0.02 M). The ratio of **4a/3a** was determined by ^1H NMR.

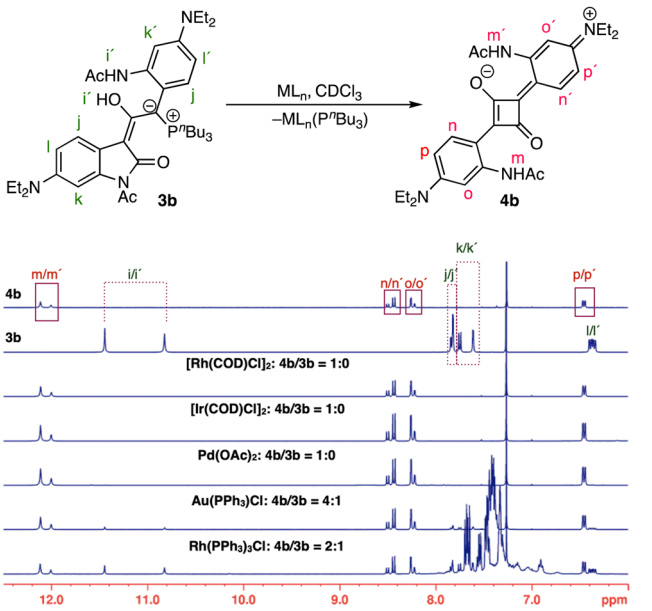

Fig. 3 Partial ^1H NMR spectra (500 MHz, $CDCl_3$) that illustrates conversion of **3b** (0.02 M) to **4b** upon addition of ML_n (0.02 M). The ratio of **4b/3b** was determined by ^1H NMR.

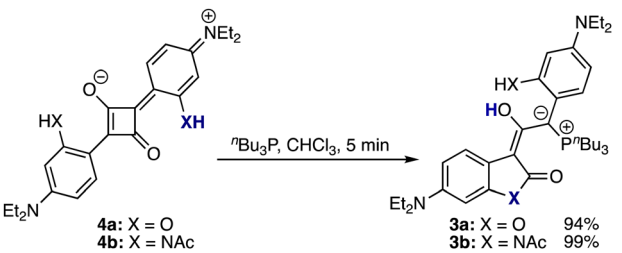

Scheme 1 Chemodosimeter **3** construction.

these complexes. For example, upon abstraction of phosphine from ylide **3**, the relatively electron rich Wilkinson's catalyst adopts an unfavorable square pyramidal geometry and the resulting phosphine-ligated Au^{I} complex a trigonal planar geometry.[6a] In contrast, the olefinic ligated Rh^{I} and Ir^{I} complexes, and electrophilic Pd^{II}, may more readily accommodate additional phosphine.[6a] Given that no reaction was observed when PPh_3 was added to **4a/b**, we suspect that those instances of

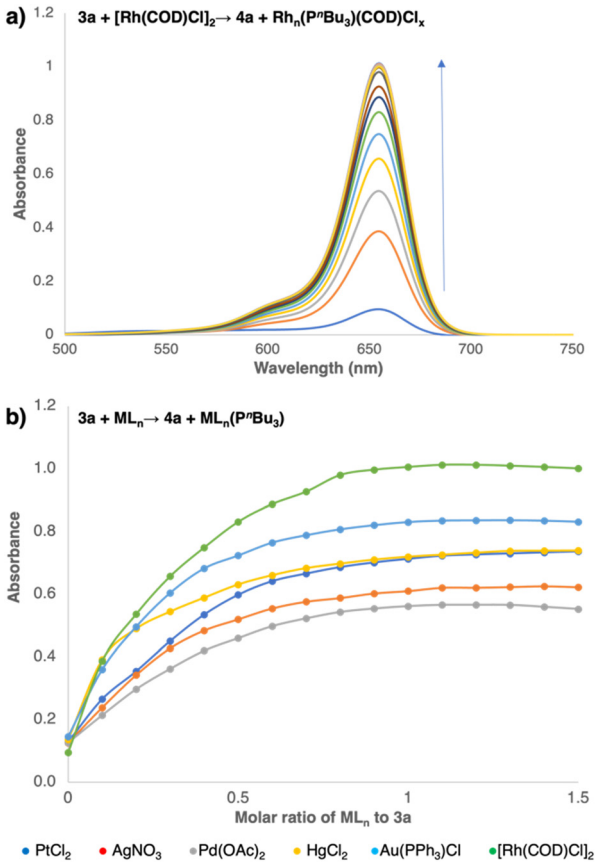

Fig. 4 (a) Appearance of **4a** absorption maxima band (λ_{max} = 655 nm) upon titration of **3a** (5.46 μM in DMSO; λ_{max} = 324 nm) with increasing amount of $[Rh(COD)Cl]_2$. (b) Titration plots showing regeneration of **4a** when separate solutions of **3a** (*ca.* 5 μM in DMSO) were titrated with $PtCl_2$, $AgNO_3$, $Pd(OAc)_2$, $HgCl_2$, $Au(PPh_3)Cl$ and $[Rh(COD)Cl]_2$.

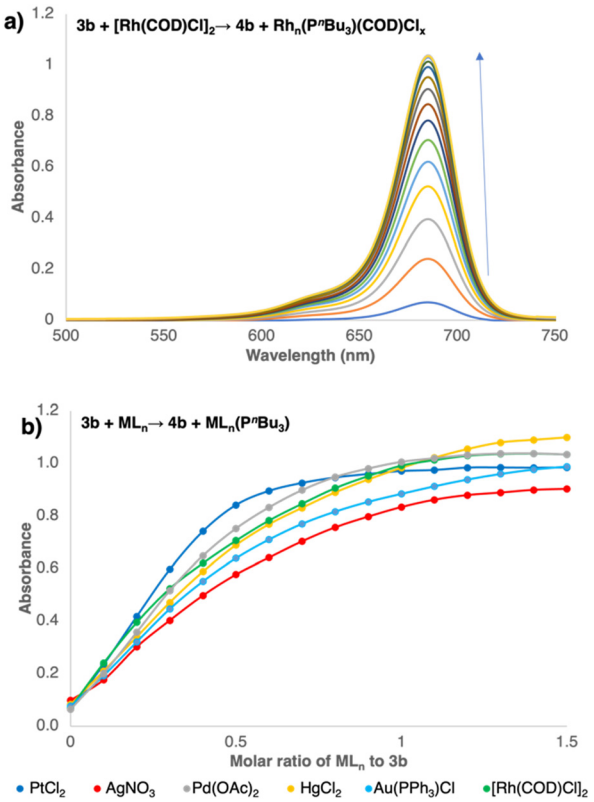

Fig. 5 (a) Appearance of **4b** absorption maxima band (λ_{max} = 685 nm) upon titration of **3b** (5.03 μM in DMSO; λ_{max} = 316 nm) with increasing amount of $[Rh(COD)Cl]_2$. (b) Titration plots showing regeneration of **4b** when separate solutions of **3b** (*ca.* 5 μM in DMSO) were titrated with $PtCl_2$, $AgNO_3$, $Pd(OAc)_2$, $HgCl_2$, $Au(PPh_3)Cl$ and $[Rh(COD)Cl]_2$.

diminished dye regeneration is unlikely due to reformation of **3a**/**b** by the reincorporation of liberated PPh_3.

Due to frequent purification challenges, detection and removal of residual transition metals can pose a hinderance, especially at low concentrations.[9–11] Employing UV-Vis spectroscopy to monitor the regeneration of dyes **4**, we tested the capability of adducts **3** to act as colorimetric chemodosimeters for metals at lower concentrations (*ca.* ∼5 μM). The addition of 0.1 equiv. (*i.e.*, 0.269 ppm) of $[Rh(COD)Cl]_2$ to adduct **3a** resulted in formation of squaraine **4a** at 2.01 μM (Fig. 4a). Increasing the concentration of $[Rh(COD)Cl]_2$ led to an increase in absorbance at 655 nm corresponding to formation of **4a**. However, the isotherm of $[Rh(COD)Cl]_2$ at 1 equiv. (*i.e.*, 2.69 ppm) plateaus with 5.41 μM free squaraine **4a**, indicating saturation of the metal center (Fig. 4b). To determine whether commonly used transition metals would result in similar UV-Vis spectroscopic responses, we examined the regeneration of **4a** from **3a** and 1 equiv. of $Au(PPh_3)Cl$, $HgCl_2$, $PtCl_2$, $AgNO_3$, or $Pd(OAc)_2$. We found that $Au(PPh_3)Cl$ plateaued to give the highest concentration of **4a** at 4.45 μM, and $AgNO_3$ and $Pd(OAc)_2$ the least in 3.24 μM and 2.97 μM, respectively.

An assessment of oxindole **3b** at 5.03 μM with $[Rh(COD)Cl]_2$ (0.1 equiv.) resulted in formation of squaraine **4b** at 1.08 μM, and increasing the concentration of $[Rh(COD)Cl]_2$ led to an increase in absorbance at 685 nm (Fig. 5a). A systematic titration provided an isotherm that plateaus upon the addition of 1 equiv. of metal and generation of squaraine **4b** at 4.40 μM (Fig. 5b). The titration of **3b** with $Au(PPh_3)Cl$, $HgCl_2$, $PtCl_2$, $AgNO_3$, and $Pd(OAc)_2$ also led to regeneration of **4b**, but unlike ylide **3a**, the amount of dye regenerated proved less distinguishable across the analytes evaluated. In contrast, the addition of $Cu(OAc)_2$, $Pb(NO_3)_2$ and $Rh(PPh_3)_3Cl$ to squaraine–phosphine ylide complexes **3** led to less **4**.[12] The formation of squaraines **4a**/**b** upon solvation, even in the absence of a metal analyte, suggests a dynamic equilibrium between **3** and **4**.

In general, the electronic and ligation structure of the metal appears to influence the extent of squaraine **4** regeneration. Electron-deficient, unsaturated metals, and those complexes bearing labile olefinic ligands, resulted in near quantitative reversion to squaraine dyes **4**. In contrast, more electron-rich metals, such as $Rh(PPh_3)_3Cl$, resulted in lower concentrations of squaraine dye **3**.[6a] Our results indicate that the metal and *ortho*-heteroatom that distinguishes between chemodosimeters **4a**/**b** influences the extent of dye regeneration. For example, while 60% conversion of benzofuranone **3a** to squaraine dye **4a** upon addition of $Pd(OAc)_2$ (1 equiv.) was observed, oxindole **3b** gave 89% of **4b**. It is conceivable that a weaker affinity of

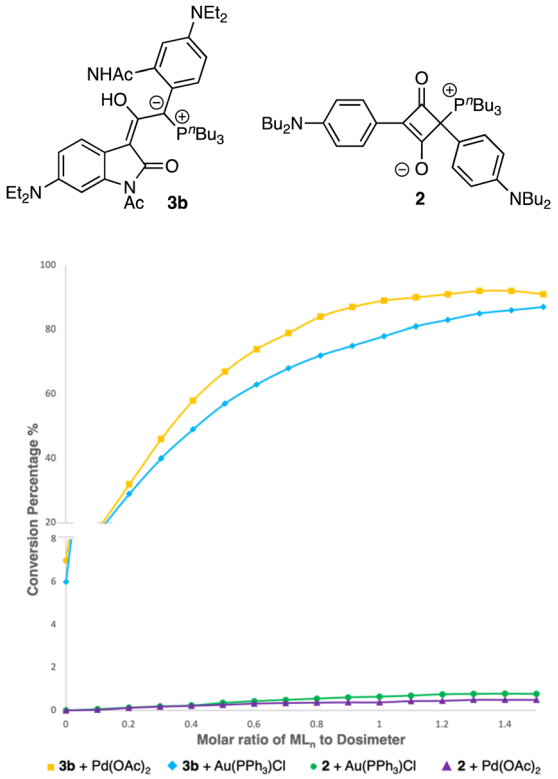

Fig. 6 Performance of chemodosimeters **3b** (*ca.* 5 μM in DMSO) and **2** (1.5 mM in DMSO), indicating conversion to **4b** and **1**, respectively, with increasing $Pd(OAc)_2$ and $Au(PPh_3)Cl$.

oxindole **4b** for P^nBu_3 is a driving force for these disparate responses.

Phosphonium ylides **3** exhibited a greater sensitivity to transition metal analytes than our previous dosimeter **2**. For example, while **3b** underwent 89% reversion to squaraine **4b** in the presence of 1 equiv. of $Pd(OAc)_2$, less than 0.4% of **1a** was obtained from squaraine–phosphine adduct **2a** (Fig. 6). Similarly, the addition of $Au(PPh_3)Cl$ (1 equiv.) resulted in 78% conversion to **4b** from **3b**, while **1a** was obtained in only 0.6% from **2a**.[6a] The ability of **3** to undergo near complete reversion may be attributed to key architectural distinctions between these two chemodosimeter designs. Dosimeter **3** is a 1,2-dipolar compound consisting of a conjugated phosphorus ylide that exhibits less double bond character than a standard ylide.[7] In contrast, the squaraine–phosphine adduct **2** is 1,3-dipolar with a kite-quadrilateral architecture that is not in conjugation with phosphorus.[6a] Upon phosphine dissociation, recapitulation of the original squaraine dye is presumably driven by rearomatization and the instability of a transient, intermediate carbene.[7,13] A primary distinction between squaraines **1** and **4** is the presence of an *ortho*-aryl heteroatom bearing a relatively acidic proton.[7] A penultimate proton transfer step is critical to driving the equilibrium between the "turned off" ylide **3** and "turned on" dye **4**, which is absent in the corresponding conversion of squaraine **1** and adduct **2**.[6a] Attractive features of this class of ylide sensors include their robust bench stability, enabling later use,[7] ability to detect metals at low concentrations, and detection of transition metal complexes not sufficiently thiophilic. While sensitivity is comparable to analogous squaraine-thiol based dosimeters, selectivity in detecting metal analytes is reduced.[6c,d]

In conclusion, a new class of squaraine-based colorimetric dosimeters, obtained from the addition of P^nBu_3 to *o*-OH or *o*-NHAc substituted dianiline squaraines, are introduced. These scaffolds are stable at rt, and exhibit enhanced sensitivity to transition metal analytes under mild conditions in comparison to our previous squaraine-derived chemodosimeters. These sensing agents underwent significant retroversion to the parent squaraines even in the presence of metal complexes exhibiting a low affinity for P^{III} at low concentrations. The stability and sensitivity of these colorimetric dosimeters suggest potential uses in detecting metals in various media. The development and examination of these dosimeters for analyte detection in different environmental conditions is underway and will be reported in due course.

Conflicts of interest

The authors have no conflicts to declare.

References

1 (*a*) S. Sreejith, *et al.*, *ACS Nano*, 2015, **9**(6), 5695–5704; (*b*) K. M. Harmatys, *et al.*, *Mol. Pharm.*, 2013, **10**(11), 4263–4271; (*c*) E. L. Cole, *et al.*, *Org. Biomol. Chem.*, 2012, **10**(30), 5769–5773; (*d*) A. G. White, *et al.*, *Bioconjug. Chem.*, 2010, **21**(7), 1297–1304; (*e*) R. R. Avirah, *et al.*, *Org. Biomol. Chem.*, 2012, **10**(5), 911–920.
2 (*a*) J. H. Yum, *et al.*, *J. Am. Chem. Soc.*, 2007, **129**(34), 10320–10321; (*b*) T. Maeda, *et al.*, *J. Phys. Chem. C*, 2018, **122**(38), 21745–21754; (*c*) G. Chen, *et al.*, *J. Mater. Chem. A*, 2015, **3**, 14517–14534; (*d*) G. Chen, *et al.*, *Appl. Phys. Lett.*, 2012, **101**, 083904; (*e*) G. Chen, *et al.*, *Phys. Chem. Chem. Phys.*, 2012, **14**, 14661–14666.
3 (*a*) A. Ajayaghosh, *Acc. Chem. Res.*, 2005, **38**(6), 449–459; (*b*) S. Das, *et al.*, *J. Phys. Chem.*, 1994, **98**(37), 9291–9296; (*c*) U. Oguz and E. U. Akkaya, *Tetrahedron Lett.*, 1997, **38**(25), 4509–4512; (*d*) K. George Thomas, *et al.*, *Chem. Commun.*, 1997, 597–598; (*e*) E. Arunkumar, *et al.*, *J. Am. Chem. Soc.*, 2005, **127**(9), 3156–3164; (*f*) D. D. Ta and V. S. Dzyuba, *Chemosensors*, 2021, **9**, 302.
4 (*a*) J. V. Ros-Lis, *et al.*, *Chem. Commun.*, 2002, 2248–2249; (*b*) J. V. Ros-Lis, *et al.*, *J. Am. Chem. Soc.*, 2004, **126**, 4064–4065.
5 (*a*) J. J. Gassensmith, *et al.*, *Org. Lett.*, 2008, **10**, 3343–3346; (*b*) J. J. Gassensmith, *et al.*, *Chem. Commun.*, 2009, 6329–6338; (*c*) E. Arunkumar, *et al.*, *J. Am. Chem. Soc.*, 2005, **127**, 3288; (*d*) E. Arunkumar, *et al.*, *Chem. – Eur. J.*, 2006, **12**, 4684.
6 (*a*) P. E. Bacher, *et al.*, *Chem. Commun.*, 2019, **55**, 3286–3289; (*b*) J. T. R. Houk, *et al.*, *Tetrahedron*, 2008, **64**, 8271–8278; (*c*) S. H. Hewage and V. E. Anslyn, *J. Am. Chem. Soc.*, 2009, **131**, 13099–13106; (*d*) J. Soto, *et al.*, *Angew. Chem., Int. Ed.*, 2005, **44**, 4405–4407.
7 P. E. Bacher, *et al.*, *Org. Lett.*, 2021, **23**(8), 2853–2857.
8 (*a*) W. P. Jencks, *Chem. Rev.*, 1972, **72**, 705; (*b*) D. A. Dougherty and E. V. Anslyn, *Modern Physical Organic Chemistry*, University Science, Sausalito, CA, 2006.
9 M. M. Reddy, *et al.*, *Pharmaceut. Reg. Affairs*, 2016, **5**, 168.
10 S. L. Buchwald, *et al.*, *Adv. Synth. Catal.*, 2006, **348**, 23–39.
11 B. Kaur, *et al.*, *Coord. Chem. Rev.*, 2018, **358**, 13–69.
12 For additional UV-Vis data on Cu(OAc)2, Pb(NO3)2, see Fig. S9, S10, S19 and S20 in the ESI†.
13 C. Wentrup, *Acc. Chem. Res.*, 2011, **44**(6), 393–404.